Geol. Mag. **147** (*4*), *2010, pp. 481–496. © Cambridge University Press 2010*
doi:10.1017/S0016756809990811

U–Pb and ^{40}Ar–^{39}Ar geochronology of the Baiyunshan gneiss (central Guangdong, south China): constraints on the timing of early Palaeozoic and Mesozoic tectonothermal events in the Wuyun (Wuyi-Yunkai) Orogen

DONG-SHENG YANG*†, XIAN-HUA LI‡, WU-XIAN LI§, XIN-QUAN LIANG§, WEN-GUO LONG§ & XIAO-LIN XIONG*

*Key Laboratory of Metallogenic Dynamics, Guangzhou Institute of Geochemistry, Chinese Academy of Sciences, P.O. Box 1131, Guangzhou 510640, China
‡State Key Laboratory of Lithospheric Evolution, Institute of Geology and Geophysics, Chinese Academy of Sciences, Beijing 100029, China
§Key Laboratory of Isotope Geochronology and Geochemistry, Guangzhou Institute of Geochemistry, Chinese Academy of Sciences, Guangzhou 510640, China

(*Received* 11 September 2009; *accepted* 26 October 2009; First published online 12 January 2010)

Abstract – Composite Sensitive High Resolution Ion Microprobe (SHRIMP) U–Pb zircon and ^{40}Ar–^{39}Ar step-heating biotite-hornblende ages are used to provide constraints on the timing and origin of the felsic gneissic rocks in the Baiyunshan Mountains region and to elucidate their tectonothermal history. SHRIMP dating and CL imaging of zircons give magmatic zircon crystallization ages between Late Ordovician and Early Silurian (*c.* 453.5 Ma, 446 Ma, and 439 Ma) for three representative felsic gneisses, suggesting that most of the Baiyunshan gneiss cannot represent basement rocks of the Cathaysia Block as previously thought. Including the present age information, a synthesis of available age data for regional Wuyun (Wuyi-Yunkai) events reflects the emergence of orogen-wide magmatism that could be syn-orogenic and have occurred mainly between 460 and 420 Ma in the South China Block. Inherited zircons are abundant, with ages clustering at late Mesoproterozoic (1189–1017 Ma) and middle Mesoproterozoic (772 Ma), which reveals that the Baiyunshan orthogneiss samples a crustal basement containing significant igneous or recycled components related to the Rodinia amalgamation and break-up. A SHRIMP date of 212 ± 12 Ma from a white rim of zircon provides evidence for metamorphic overprinting of an Indosinian tectonothermal event on the Baiyunshan gneiss. Incremental heating experiments with six biotite samples and one hornblende sample from a variety of metamorphic rocks yielded two distinct ^{40}Ar–^{39}Ar age groups: 150–155 and 94–98 Ma. The older ages are similar to zircon U–Pb dates for widespread granitic intrusions in central Guangdong. We attribute them to Late Jurassic magmatism-induced thermal resetting of the biotite K–Ar system. On the other hand, the younger age group is interpreted to record either cooling through the biotite closure temperature of ~ 300–350 °C or a second resetting of biotite Ar isotopes at *c.* 94–98 Ma due to contemporaneous magmatic activity. Our present age data suggest that the Maofengshan orthogneiss was exhumed to 8 to 10 km crustal levels at *c.* 150 Ma, whereas the eastward components of gneissic rock masses appear to have passed upward through the same crustal depth synchronously or later (by *c.* 94 Ma). Exhumation of middle crustal-level rocks in the study area since *c.* 155 Ma is roughly coeval with exhumation of gneissic rocks from elsewhere in the Wuyun Orogen, suggesting a large-scale mechanism for the exhumation pulse related to the Yanshanian extensional tectonic regime.

Keywords: Baiyunshan, gneiss, U–Pb, ^{40}Ar–^{39}Ar, geochronology, south China.

1. Introduction

The South China Block comprises the Archaean–Proterozoic Yangtze Block and the Palaeoproterozoic to Mesoproterozoic Cathaysia (or Huanan) Block (Fig. 1; Li, 1997, 1998; Chen & Jahn, 1998; Gao, Lin & Qiu, 1999; Shen *et al.* 2000). It is a consequence of a series of intercontinental and intracontinental collisions and deformations that have occurred since Proterozoic times (e.g. Li & McCulloch, 1996; Charvet *et al.* 1996; Li, 1998). The early Palaeozoic orogen (Fig. 1) in south China occupies most or part of the southern provinces of mainland China and could have extended into the Korean peninsula and the Indochina Block (Guo *et al.* 2009; Li *et al.* 2010 and references therein). Its formation may be linked to interactions between the Cathaysia margin of the South China Block and the Australian–Indosinian margin of Gondwanaland that rotated clockwise during Ordovician–Silurian times (Li, 1998; Li & Powell, 2001). Therefore, knowledge of the orogen, including its nature, extent and tectonothermal evolution, is

†Author for correspondence: yds1019@gig.ac.cn

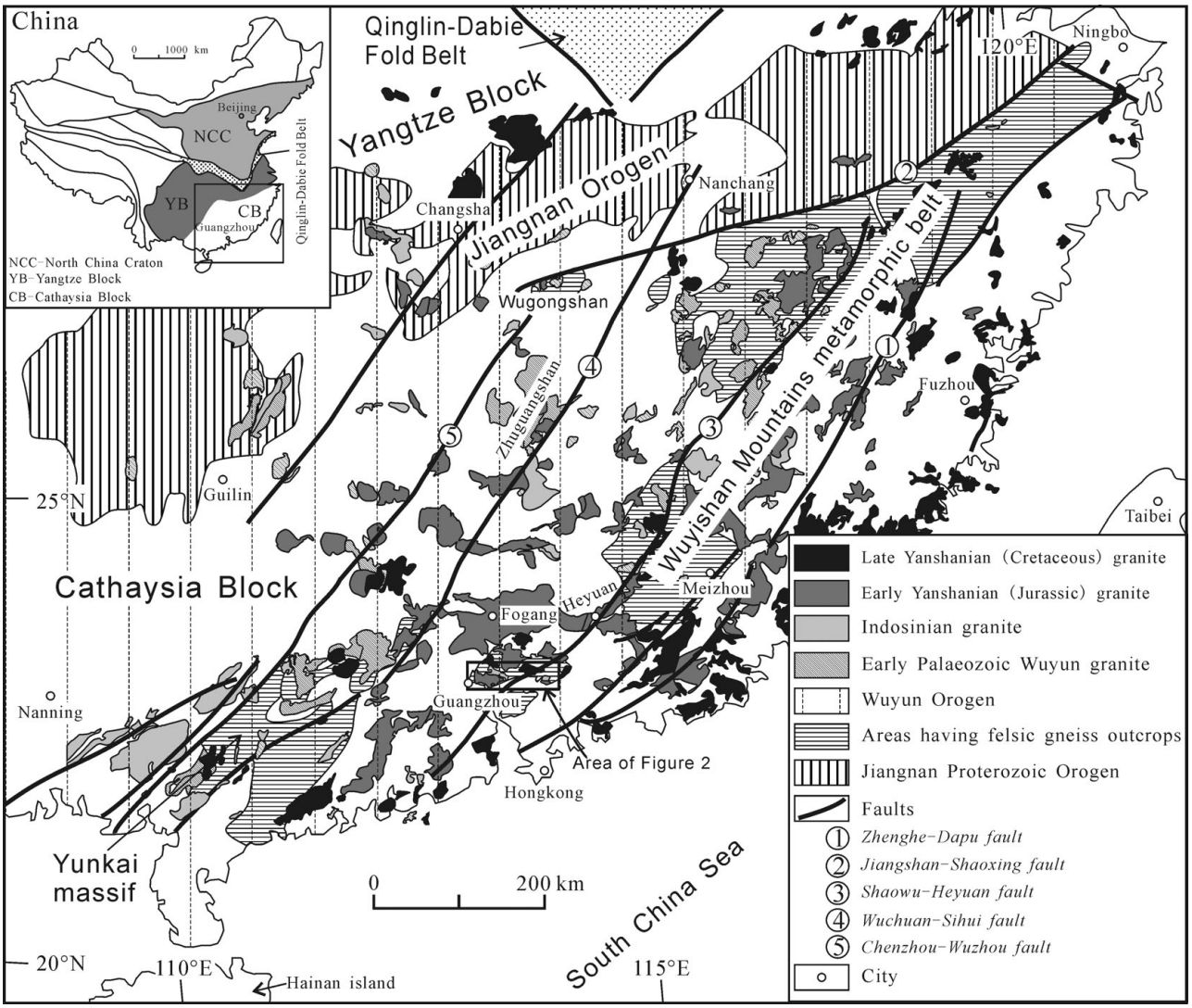

Figure 1. Tectonic sketch map of the early Palaeozoic Wuyun (Wuyi-Yunkai) Orogen within the South China Block (the combination of the Yangtze and Cathaysia blocks), with regional distribution of the felsic gneisses and (post-)Wuyun granites. Box indicates the location of Figure 2. Modified from Li (1998), Zhang & Wu (2002) and Sun (2006). Inset shows position of the map field area in China.

essential to understanding the formation of East Asia and to constraining early Palaeozoic global geodynamics and palaeography (Shu, 2006; Li *et al.* 2010).

The early Palaeozoic orogenic event in south China has been referred to as the South China Caledonian Orogeny since its recognition in the 1960s (e.g. Huang, 1960; Ren, 1964; Guo, Yu & Shi, 1965). In the western geological literature, however, the word 'Caledonia' is commonly employed to describe a geographically restricted orogeny that took place within, and on the borders of, the Iapetus Ocean (McKerrow, Niocaill & Dewey, 2000). To avoid confusion, we here use the term 'the Wuyun (Wuyi-Yunkai) Orogeny (and for the orogen, the Wuyun Orogen)', recommended by Li *et al.* (2010), to encompass all the tectonic events affecting the South China Block in the early Palaeozoic (Late Ordovician? to Silurian).

Inliers of felsic gneissic rocks are common in the Wuyun Orogen. They are traditionally considered to be uplifted Precambrian (pre-Sinian *c.* 680 Ma) fragments of continental crust that represented the basement of the Cathaysia Block (e.g. Shu, 2006). Geochronology has constrained the origin and evolution of the felsic gneisses with unprecedented resolution in some parts of the Yunkai massif and the Wuyishan metamorphic belt (Fig. 1; Table 1), the two best-studied areas with abundant occurrences of gneissic rocks. It is now realized that the gneiss exposed in the Wuyishan belt may mostly represent Proterozoic basement rocks which experienced extensive overprinting by high-grade metamorphism, migmatization and anatexis during the Wuyun Orogeny (Ye *et al.* 1994; Shu *et al.* 1999; Yu *et al.* 2005; Wan *et al.* 2007; Liu *et al.* 2008; Zeng *et al.* 2008; Li *et al.* 2010). For most of the felsic gneisses from the Yunkai massif in western Guangdong, however, several recent high-precision geochronological studies indicate that they are actually of Caledonian-aged anatectic origin (Wang *et al.* 2007*a*; Peng *et al.* 2006). This present situation highlights the necessity of re-evaluating the gneisses of the Baiyunshan Mountains region in

https://doi.org/10.1017/S0016756809990811 Published online by Cambridge University Press

Table 1. Summary of published high-precision geochronological data for the Wuyun Orogen

Locations and sample collected	Dated material (methodology)*	Interpretation	Age (Ma)	References
Wuyishan metamorphic belt				
Gneissic amphibolite from the Chencai Complex	Hornblende (C)	Retrograde metamorphic/ cooling age	415 ± 3	Ye *et al.* 1994
Cizhu gneissic granite, Yiyang county	Muscovite (C)	Ductile deformation associated with shear zones	421 ± 8	Shu *et al.* 1999
Hudiejie marble, Zhenghe county	Muscovite (C)	Metamorphic event	391 ± 3	
Taoxi Formation (monzonitic gneiss)	Zircon rims (B)	Granulite-facies metamorphism	443 ± 10	Yu *et al.* 2005
	Mantles of sector-zoned zircons (B)	An episode of Caledonian anatexis	444 ± 5	
Mayuan Group, sillimanite-biotite gneiss	Zircon rims (A)	High grade metamorphism	458 – 425	Wan *et al.* 2007
Granodiorite neosome from Tianjingping migmatite	Zircon (D)	Emplacement age	447 ± 2	Zeng *et al.* 2008
Migmatites and related granites in northwestern Fujian	Zircon (B)	Age of migmatization and magmatic crystallization	437 – 441	Liu *et al.* 2008
Daojiuwan Formation, metagabbro Formation, gneissic granite Xiawuzhai Mayuan Formation, amphiobolite and gneiss Longyou Complex, granitic gneiss	Zircon (A)	High-grade metamorphic age	443 – 460	Li *et al.* 2009
Daojiuwan Formation, migmatite Xiawuzhai Formation, gneissic granite Tianjingping granitic leucosome Sibao granite Weipu granite	Zircon (A)	Syn- to late orogenic melt age	432 – 452	
Daojiuwan Formation, metagabbro Xiawuzhai Formation, gneissic granite Wannian Group, mica schist	Hornblende(C) Biotite (C) Muscovite (C)	Retrograde metamorphic/ cooling age	420 – 438	
Yunkai massif				
Leucosome from Gaozhou migmatite	Single zircon (D)	Migmatization	394 – 449	Wang, Tu & Sun, 1999
Granitic orthogneiss	Zircon (A and B)	Emplacement age	421 – 441	Wang *et al.* 2007*a*
Wugongshan area				
Shanzhuang granodiorite	Zircon (D)	Emplacement age	461 ± 2	Lou *et al.* 2005
Zhangjiafang biotite granite	Zircon (D)	Emplacement age	428 ± 1	
Wugongshan granite	Zircon (D)	Emplacement age	428 – 462	
Zhuguangshan area				
Tanghu granite	Zircon (D)	Emplacement age	434 ± 2	Li *et al.* 1989
Guidong granodiorite	Zircon (D)	Emplacement age	427 ± 3	Li, 1994
	Hornblende (C)	Folding event	371 ± 1	
Migmatite	Zircon (A)	Migmatization	425 – 470	Xu *et al.* 2005
Laojunshan–Song Chay metamorphic dome				
Song Chay orthogneiss	Zircon (D)	Emplacement age	428 ± 5	Roger *et al.* 2000
Dulong metamorphic complex	Zircon (A)	Emplacement age of the granitic protolith	436 – 402	Yan, Zhou & Wang, 2006
Laojunshan granites	Zircon (A)	Emplacement age	442 – 418	Guo *et al.* 2009

*Dating method: A – SHRIMP U–Pb; B – LA-ICPMS U–Pb; C – ^{40}Ar–^{39}Ar; D – TIMS U—Pb.

central Guangdong. This region has excellent surface exposures of felsic gneisses and offers an important spatial connection between the Yunkai massif to the southwest and the Wuyishan belt to the northeast (Fig. 1). Nevertheless, there are few published age determinations for this region. Existing geochronological data include several Meso-Neoproterozoic and early Palaeozoic single-zircon U–Pb and Pb–Pb evaporation ages (Wu, 1991; Liu & Zhuang, 2003), as well as a middle Carboniferous K–Ar age of 312 Ma (GBGMR, 1988), and no analytical details were provided from these early studies.

We present here for the first time reliable geochronological data for the granitic gneiss and some other metamorphic rocks exposed in the Baiyunshan region (corresponding geographically to Guangzhou, the largest city of southern China, and its surrounding counties townships). Based on composite Sensitive High Resolution Ion Microprobe (SHRIMP) U–Pb zircon and ^{40}Ar–^{39}Ar biotite-hornblende dating, this paper aims to provide constraints on the timing and origin of the high-grade metamorphic rocks and to unravel their tectonothermal history. The time-scale used in this study is GTS2004 (Gradstein *et al.* 2004).

2. Geological setting

2.a. Regional setting

The early Palaeozoic Wuyun Orogen corresponds spatially to the area of the Neoproterozoic Nanhua failed rift system that developed within the South China

https://doi.org/10.1017/S0016756809990811 Published online by Cambridge University Press

Block (Li, 1998; Wang & Li, 2003). The former Nanhua rift represents a tectonically weak zone that was a domain of extremely active tectonics and magmatism during the Wuyun Orogeny (Wang *et al.* 2007*a*). This orogeny led to an angular unconformity between the folded early Palaeozoic basement and the Upper Devonian conglomerate and coarse sandstone in the entire south China area (Shu, 2006).

The tectonic environment and geodynamic driving force for the Wuyun Orogeny is still poorly known. It has been claimed to be genetically related to oceanic subduction and subsequent continental or arc collisions or post-collision lithospheric delamination (Guo *et al.* 1989; Hsü, 1994; Charvet *et al.* 1996; Peng *et al.* 2006). The presently available geological data demonstrating that no evidence of a major early Palaeozoic ocean basin is evident in south China, however, tend to argue for an intracontinental tectonic regime for the Wuyun Orogeny (this does not preclude the possibility of the existence of a small oceanic basin; Li, 1998; Li *et al.* 2010; Wang & Li, 2003; Wang *et al.* 2007*a*). These data include: (1) the Wuyun Orogeny was accompanied by widespread granitoid intrusions of middle Palaeozoic age, coupled with the absence of coeval (arc) volcanic rocks (Shu, 2006; Sun, 2006); (2) geochemical and geochronological data presented in the literature reveal that the Wuyun granites are mostly anatectic products of Precambrian continental crust, with little evidence for material contribution from a subducting oceanic plate (e.g. Jahn, Zhou & Li, 1990; Chen & Jahn, 1998; Zeng *et al.* 2008; Guo *et al.* 2009); and (3) sedimentary facies distribution shows that an apparent exchange of sedimentary sources occurred between the Yangtze and Cathaysia blocks on both sides of the failed Nanhua basin in Cambrian times when the basin was at its broadest (Liu & Xu, 1994; Li, 1998; Li *et al.* 2010).

In southern China, the Wuyun Orogen also almost completely overlaps in space with a tectonomagmatic zone of Late Permian through Triassic age ('Indosinian period') (Fig. 1). This is partly due to the similar intracontinental tectonic setting of the Wuyun and Indosinian orogenies (Wang *et al.* 2007*a*,*b*).

During the late Mesozoic ('Yanshanian period'), the palaeo-Pacific plate was somehow subducted under the Eurasian plate (Jahn, Zhou & Li, 1990; Charvet, Lapierre & Yu, 1994; Lapierre *et al.* 1997; Zhou & Li, 2000; Li & Li, 2007; Li *et al.* 2007), resulting in a widespread continental margin magmatic zone, as much as > 1000 km wide and > 3000 km long, along the eastern margin of China. It is now widely accepted that the Mesozoic Yanshanian magmatism in eastern China is attributable to intracontinental lithospheric extension in response to asthenospheric mantle upwelling (e.g. Li, 2000; Wang *et al.* 2003*c*; Zhou *et al.* 2006). The broad Yanshanian magmatic zone overprints all previous events in the South China Block (Fig. 1).

Exposures of possible Wuyun-aged rocks within the South China Block are mainly restricted to the Yunkai massif, the Wuyishan Mountains metamorphic belt (in this work the belt is defined to cover the Mountains region and the Chencai Complex and adjacent regions because of age similarity in the metamorphic rocks and their protoliths; Li *et al.* 2010), the Baiyunshan Mountains region, the Zhuguangshan and Wugongshan areas, respectively, at the Jiangxi–Hunan–Guangdong and Jiangxi–Hunan provincial boundaries, all of which are located in the Cathaysia Block (Fig. 1). Additionally, in the Jiangnan Proterozoic Orogen, which is classically regarded as the southern edge of the Yangtze Block (Charvet *et al.* 1996), particularly in the Jiangxi and Hunan segments of the belt, deformation and magmatism associated with late early Palaeozoic compressive reworking has been well documented (Xu, Guo & Shi, 1992; Deng & Zhang, 1996). Also, in recent years some Wuyun granites have been reported in the Laojunshan–Song Chay metamorphic dome on the border between southeastern Yunnan (China) and northern Vietnam (Roger *et al.* 2000; Yan, Zhou & Wang, 2006; Guo *et al.* 2009). The main sectors of the Wuyun Orogen are roughly delimited to the north by the Jiangshan–Shaoxing fault zone and to the southeast by the Zhenghe–Dapu fault zone (Fig. 1). An early Neoproterozoic ophiolitic complex zone occurs along the Jiangshan–Shaoxing fault; it is therefore thought that the latter marks the collisional suturing between the Jiangnan ancient arc and the Cathaysia Block (Jinning or Grenville Orogeny: Shui *et al.* 1986; Chen *et al.* 1991; Zhou & Zhu, 1992; Li & McCulloch, 1996). The tectonics of the Zhenghe–Dapu fault zone, however, remains an interesting challenge. A suite of metavolcanic rocks with mafic and ultramafic small intrusions occurs along the fault zone, which has recently been dated at *c.* 1750 Ma (Sm–Nd method; Wang *et al.* 2003*a*), at variance with the viewpoint of Guo (1989) that these meta-igneous rocks are a Caledonian-aged ophiolite assemblage.

The structural and tectonostratigraphic region between the Jiangshan–Shaoxing and Zhenghe–Dapu fault zones is characterized by the presence of inliers of felsic gneisses which are commonly considered to be remnants of microcontinental fragments of the Cathaysia Block (Fig. 1). The gneissic rocks are mainly distributed along several coastal provinces comprising Zhejiang, Fujian and Guangdong, generally metamorphosed to the greenschist to upper amphibolite facies. Locally in the Gaozhou–Yunlu zone of the Yunkai massif and in the southern part of the Wuyishan Mountains, felsic gneisses also record low-pressure (4–5.2 kbar; Chen, 1992; Zhou *et al.* 1994*b*) or high-pressure (~ 1.1 GPa; Yu *et al.* 2003) granulite-facies metamorphic conditions. Widespread regional metamorphism leading to most of the felsic gneissic rocks has been ascribed principally to the early Palaeozoic Wuyun evolution (GBGMR, 1988; Chen, 1992; Zhang & Wu, 2002; Yu *et al.* 2005; Xu *et al.* 2005; Wan *et al.* 2007; Li *et al.* 2010), although alternative interpretations suggest that the Wuyun-aged igneous rocks within the Yunkai massif might

https://doi.org/10.1017/S0016756809990811 Published online by Cambridge University Press

have been metamorphosed to gneissic rocks during Indosinian reactivation (Wang *et al.* 2007*a*).

2.b. Local geology

In the the eastern and northern parts of the Baiyunshan region (Figs 1, 2), metamorphic rocks composed of predominantly felsic gneiss with minor schist, quartzite, metasandstone and migmatite are widespread, whereas in other areas the geology is largely dominated by Cenozoic sediments. Metamorphic basement rocks are unconformably overlain by or in fault contact with unmetamorphosed Devonian to Cenozoic sedimentary cover rocks. The felsic gneiss of Baiyunshan, once considered to be Wuyun intrusive rocks (e.g. the rocks cropped out in the Maofengshan area and to the northwest of the Xintang–Luofushan fault) or Lower Palaeozoic metasediments (Geological Map of Guangzhou, 1968; Geological Map of Heyuan, 1968), is now interpreted as Sinian or Meso- and Neoproterozoic rocks (GBGMR, 1988; Liu & Zhuang, 2003). Pervasive foliation in the gneisses is generally concordant with the country rock structures, defined principally by discontinuous biotite flakes (Fig. 3) and, as a whole, oriented in a northeasterly direction.

The minerals included in gneisses are diagnostic of the amphibolite-facies mineral assemblage (plagioclase + quartz + biotite ± garnet ± hornblende ± K-feldspar). Thin discontinuous lenses of massive amphibolite are found to occur in parts of the Baiyunshan gneiss. Retrograde alteration shown by variably chloritized biotite and sericitized feldspar has been locally observed. In some locations, leucogranites occur more or less as < 0.5 m thick, concordant, or slightly discordant veins that are folded or undeformed. Petrographically, the leucogranites consist of quartz, plagioclase, K-feldspar, biotite and accessory minerals, and attest to anatexis during low-pressure–high-temperature metamorphism.

The Baiyunshan metamorphic region is intruded by extensive Mesozoic granitic plutons (dominantly early Yanshanian), and in the north it adjoins the EW-trending Fogang batholith in the southern segment of the famous Nanling Ranges granitoids. Zircons from one granite sample collected near the town of Luogang (Fig. 2) have been dated by LA-ICPMS at 153 ± 6 Ma (D. S. Yang, unpub. data). This age broadly resembles that of the Fogang I-type and Nankunshan A-type granites belonging to the Fogang batholith (Liu *et al.* 2005; Li *et al.* 2007). The regional magmatic event of the same age has been hypothesized to be the result of foundering of an early Mesozoic subducted flat-slab beneath the SE China continent (Li *et al.* 2007).

A significant normal fault system, herein informally named the Xintang–Luofushan fault zone, has been recognized in the area of investigation which merges easterly into the crustal-scale Heyuan (–Shaowu) fault and extends from Sanshui city, approximately 30 km west of Guangzhou, through Xintang to Boluo and Mt Luofushan (Figs 1, 2). The fault is thought to be

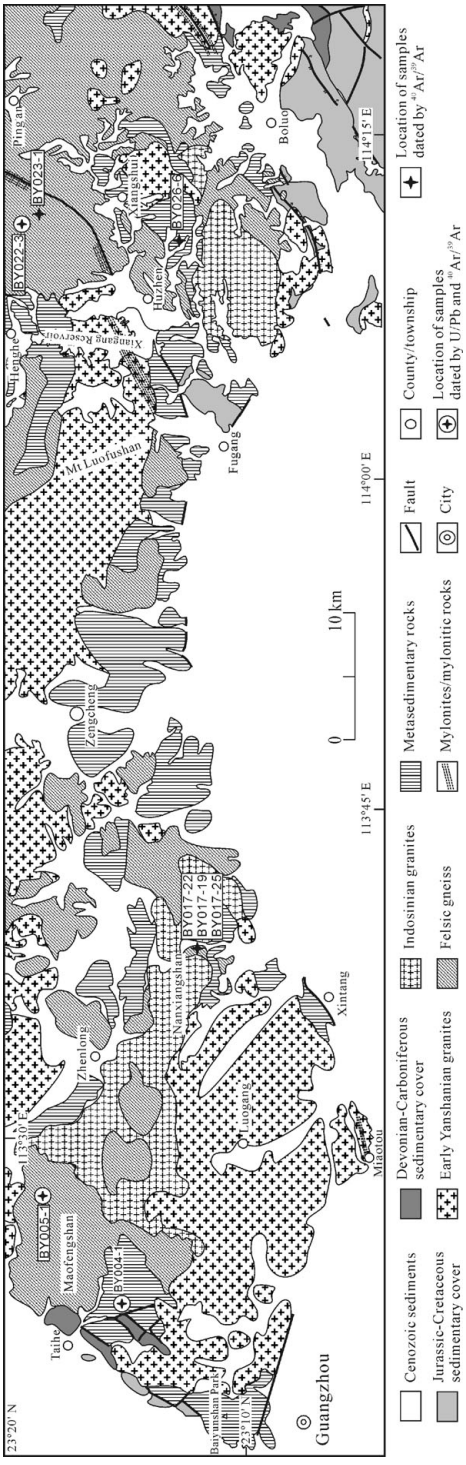

Figure 2. Geological map of the eastern and northeastern parts of the Baiyunshan region showing numbers and sites of the samples used in this study. Other parts of this region are predominantly filled by Cenozoic sediments and therefore omitted. The map is compiled from earlier published geological maps (Geological Map of Guangzhou, 1968; Geological Map of Heyuan, 1968). Note that the previously mapped metasedimentary rocks consist of felsic gneiss, schist, quartzite and metasandstone, but much of the 'paragneiss' may well be orthogneiss based on our geochronological result from sample BY004-1 (see text for details).

https://doi.org/10.1017/S0016756809990811 Published online by Cambridge University Press

an extensional detachment fault which was initiated in Late Jurassic times (Wu, Liu & Liao, 2001); it strikes variably from ESE 100° to ENE 70–80° and dips moderately south or southwest. Along the fault trace, mylonites and mylonitic rocks derived from granitic and gneissic protoliths are exposed at or near Xintang, the Xiangang Reservoir and Boluo (Fig. 2), and the production of the mylonites could be due to the detachment motion (Wu, Liu & Liao, 2001). The timing of ductile deformation on the shear zone is constrained at Xintang by ^{40}Ar–^{39}Ar dates of 217 Ma and 172 Ma obtained for biotite (Zou *et al.* 2001). However, our unpublished geochronological data (see above) suggest that all or part of the observed deformation should have occurred later than 155 Ma because of a cross-cutting relationship of the Yanshanian Luogang granite with the shear zone.

3. Analytical methods

3.a. Zircon U–Pb dating

Zircons were concentrated using standard gravimetric and magnetic separation techniques. Representative grains were then extracted by hand-picking under a binocular microscope. Zircons from the samples described below were cast, along with fragments of a standard zircon (TEMORA), in an epoxy mount. The mount was polished with diamond compound to reveal zircon mid-sections, and all sectioned zircons were documented with transmitted and reflected light micrographs as well as cathodoluminescence (CL) images to identify their internal structures (including growth zoning, recrystallization/overgrowth, alteration and cracks) and select spots for analysis. The *in situ* U–Pb ages were obtained with the use of the SHRIMP II ion microprobe at the Beijing SHRIMP Centre, Chinese Academy of Geological Sciences. Operating conditions and data processing procedures were similar to those described in detail by Williams (1998). Calibration concentrations of U and Th were based on analyses of zircon SL13. Isotopic compositions were calibrated by replicate analyses of the TEMORA standard (*c.* 417 Ma, $^{206}Pb/^{238}U = 0.06683$; Black *et al.* 2003). Final ^{204}Pb-corrected ratios and ages are reported with 1σ analytical errors (68 % confidence levels), as are the error ellipses shown in the concordia diagrams presented below. Nonetheless, calculated weighted mean ages in the text are presented at 95 % (2σ) confidence limits.

3.b. ^{40}Ar–^{39}Ar dating

High-purity (> 99 %) mineral separates of biotite and hornblende were obtained by crushing, washing in de-ionized water, sieving to 40 to 80 meshes, and hand-picking. The amount of biotite used for analysis was between 0.2 and 0.3 mg, whereas 5 mg was used for hornblende. The mineral concentrates were wrapped in aluminium foil packets, encapsulated in sealed quartz vials, and irradiated in a nuclear reactor at the China Institute of Atomic Energy in Beijing. Variations in the flux of neutrons along the length of the irradiation assembly were monitored with mineral standards DRA1 (sanidine with age of 25.26 ± 0.07 Ma) and ZBH25 (biotite with age of 132.9 ± 1.3 Ma). The two standards are very homogeneous and have excellent reproducibility (Wijbrans *et al.* 1995; Sang *et al.* 2006).

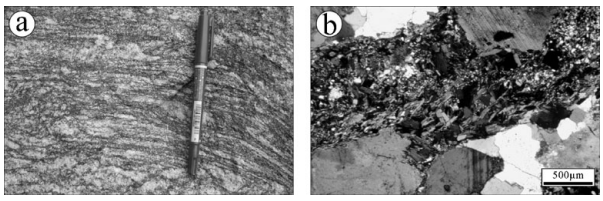

Figure 3. Examples of biotite-defined gneissic fabric developed within the Baiyunshan gneiss. (a) Field photograph taken at the site sampling BY004-1. (b) Crossed nicols photomicrograph of sample BY005-1. See Figure 2 for sample location.

Following fast neutron irradiation, argon isotopes were measured at the GIG-CAS Ar/Ar Isotope Laboratory. Mineral separates were step-heated in 12 to 18 steps at incrementally higher powers in the defocused beam of a 50W CO_2 laser (MIR10, ®New Wave Research, Inc.). The gas evolved from each step was analysed by a high sensitivity GV5400 mass spectrometer equipped with an ion-counting electron multiplier. Details of analytical and data reduction procedures can be found in Qiu & Wijbrans (2006) and Qiu (2006). Ages for individual temperature steps were calculated by assuming an initial atmospheric $^{40}Ar/^{36}Ar$ ratio equal to 295.5 (Steiger & Jäger, 1977). Errors quoted on the ages and Ar isotope ratios are at the 2σ levels. The ^{40}Ar–^{39}Ar dating results were treated and calculated using the ArArCALC software package (http://earthref.org/tools/ararcalc/index.html) (Koppers, 2002).

4. SHRIMP U–Pb zircon geochronology

Mineralogically and structurally similar gneissic rocks occur in large areas of Baiyunshan. In this study, U–Pb SHRIMP dating of zircon crystals was carried out on three felsic gneiss samples (BY005-1, BY022-3 and BY004-1) which are foliated. Sample locations are indicated in Figure 2. The dated rocks include ortho- and paragneisses previously mapped and are typical for the gneiss within the Baiyunshan region. Combined with zircon CL images, a number of different zircon fractions from these samples were targeted to constrain the origin, age and tectonothermal overprinting. Efforts were made to avoid analysing areas with cracks and inclusions. Figure 4 shows morphologies and CL zoning patterns of some representative zircon crystals, as well as locations of the analytical pits and the resulting apparent ages. Isotopic data for each sample are presented in online Appendix Table A1 at http://journals.cambridge.org/geo and plotted in concordia diagrams (Fig. 5a–d). The results of the age determinations, along with ^{40}Ar–^{39}Ar age data (see next Section), are summarized in Table 2. In

https://doi.org/10.1017/S0016756809990811 Published online by Cambridge University Press

Table 2. Summary of U–Pb and ^{40}Ar–^{39}Ar age data obtained in this study

		SHRIMP U–Pb zircon age (Ma)			^{40}Ar–^{39}Ar mineral age (Ma)*	
Sample	Lithology	Magmatic crystallization	Inherited cores	Metamorphic rim	Plateau	Isochron
BY004-1	Gneiss	446 ± 7	1017–1030	212 ± 12		
BY005-1	Gneiss	453.5 ± 7.8	751–1190, 3027		148.8 ± 0.5 (Bi)	150.3 ± 4.3 (Bi)
BY022-3	Gneiss	439 ± 9			93.8 ± 0.3 (Bi)	94.0 ± 0.1 (Bi)
BY017-22	Amphibolite				172 ± 3 (Hb)	155 ± 4 (Hb)
BY017-25	Gneiss				97.7 ± 0.4 (Bi)	97.5 ± 0.5 (Bi)
BY017-19	Leucogranite				95.9 ± 0.4 (Bi)	96.3 ± 1.2 (Bi)
BY023-1	Gneiss				93.2 ± 0.3 (Bi)	93.6 ± 0.5 (Bi)
BY026-6	Micaschist				–	–

*Abbreviations of minerals dated: Hb – hornblende, Bi – biotite.

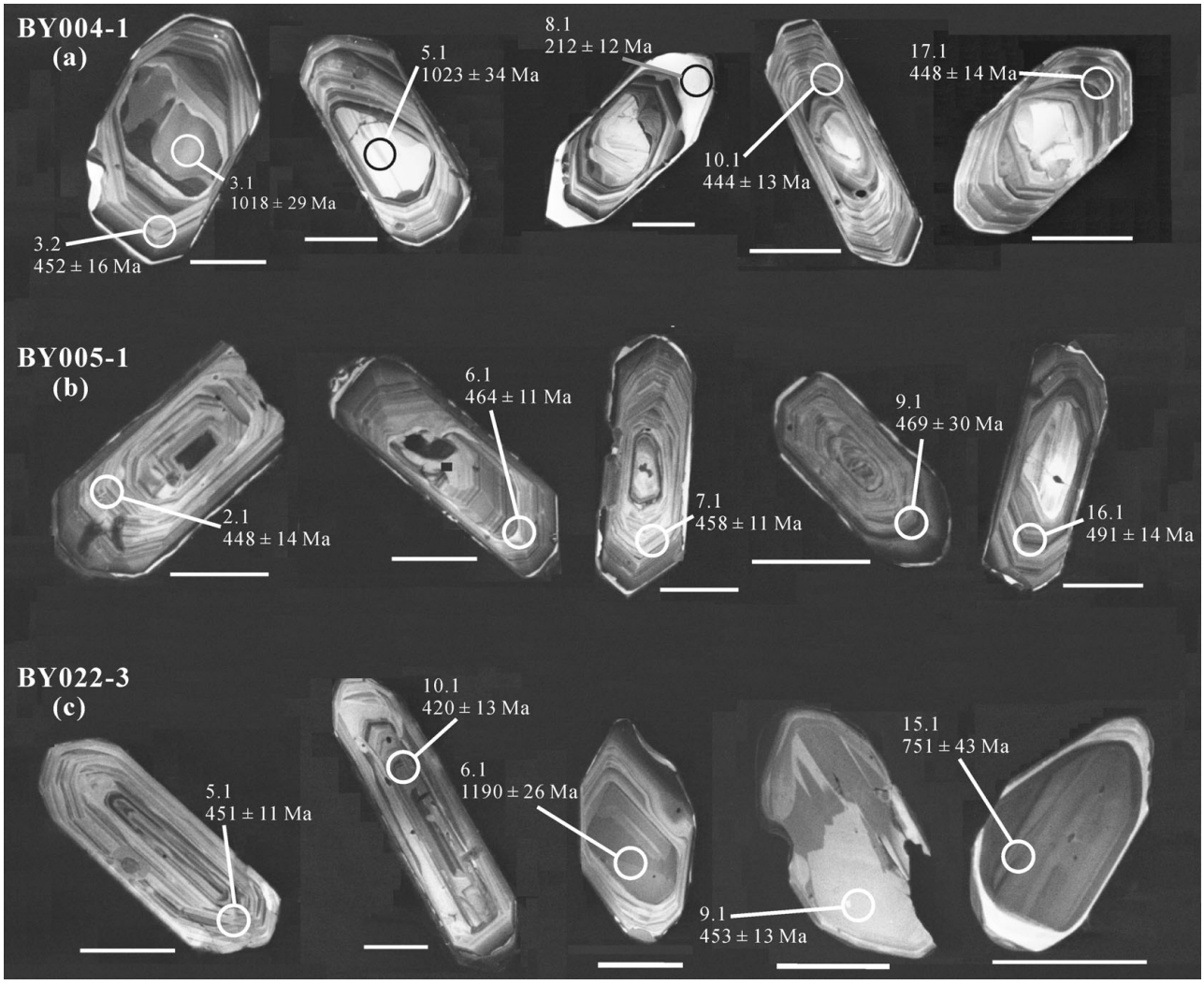

Figure 4. Representative cathodoluminescence (CL) images of zircon grains from dated felsic gneiss samples. Small circles point to analytical pits, in all cases about a 30 μm diameter; grain and spot numbers, and resulting $^{206}Pb/^{238}U$ ages (±1σ uncertainties) are indicated and correspond to those listed in online Appendix Table A1 at http://journals.cambridge.org/geo. All scale bars equal 100 μm. Note rounded cores with or without platy zoning that yield old ages in samples BY004-1 and BY022-3.

this investigation, zircons younger than *c.* 1.2 Ga were dated using the $^{206}Pb/^{238}U$ age, whereas older ones used the $^{207}Pb/^{206}Pb$ age.

4.a. Sample BY004-1: granitic biotite gneiss

Sample BY004-1 is from an abandoned quarry of felsic gneiss in the northwestern portion of the study area, about 15 km northeast of Baiyunshan Park (23°15′04″N/113°22′09″E) (Fig. 2). It consists of approximately 46 % plagioclase ($An_{35–40}$), 35 % quartz, 18 % biotite and 1 % K-feldspar. Foliation of the investigated gneiss is moderate to weak, defined principally by discontinuous, subparallel alignment of biotite flakes (Fig. 3a). Quartz occasionally shows undulatory extinction and sutured margins or is polycrystalline in form, features which suggest post-crystallization deformation.

https://doi.org/10.1017/S0016756809990811 Published online by Cambridge University Press

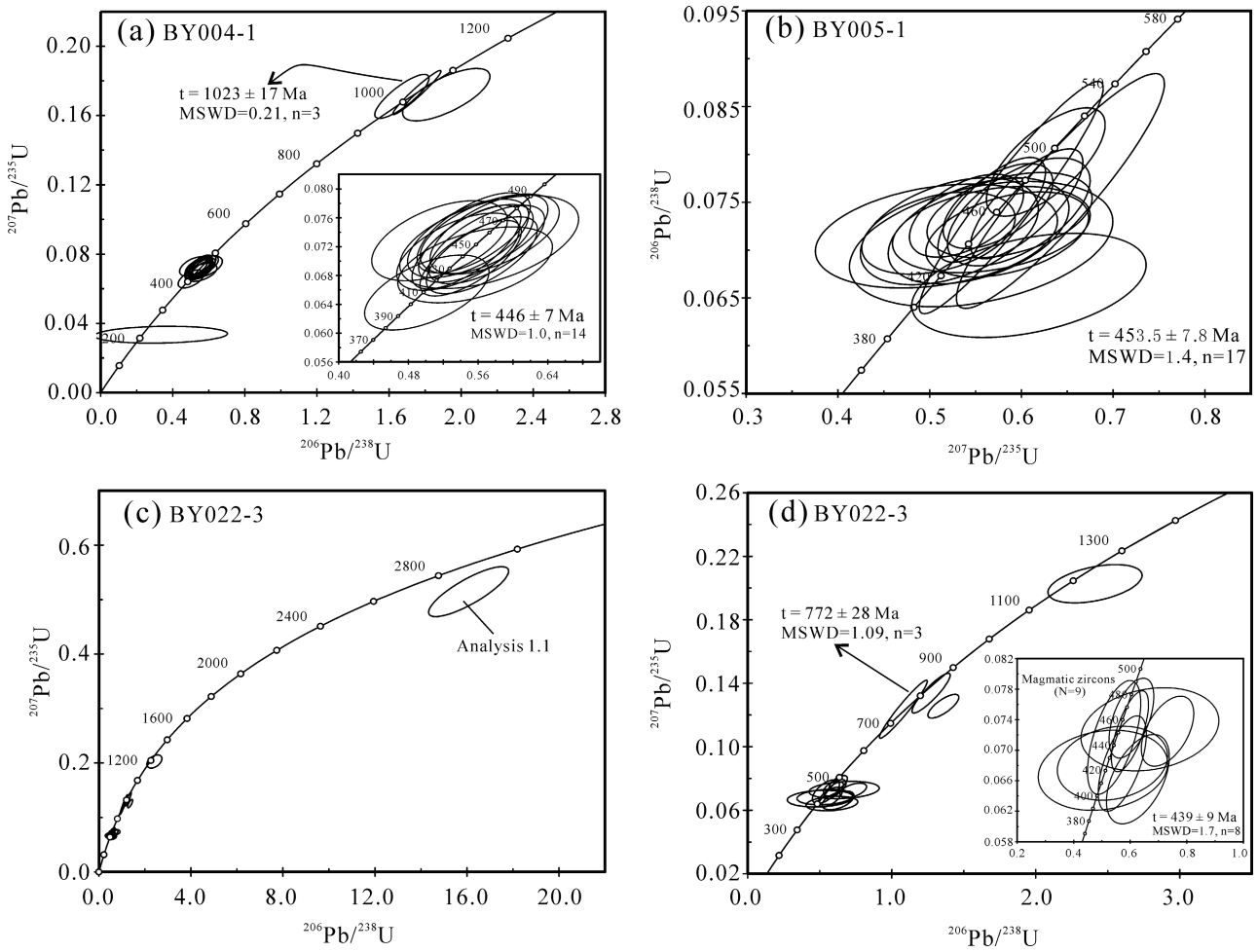

Figure 5. Concordia diagrams showing U–Pb SHRIMP data (online Appendix Table A1) for zircons from dated felsic gneiss samples (a) BY004-1; (b) BY005-1 (Maofengshan pluton) and (c, d) BY022-3. Data are shown as 1σ error ellipses, but calculated mean ages are ±2σ.

The sample yielded a single population of elongate (2:1–4:1), clear, colourless to slightly brown, euhedral zircon, characteristic of magmatic origin (Hanchar & Miller, 1993; Da Silva *et al.* 2000). The zircons range in size between 100 and 450 μm. Relict cores with or without planar zoning are often present (Fig. 4a). Most zircons are overgrown by thin white rims that were usually too small to allow analysis and clearly identify their origin; however, scanned CL imaging presents a grain with a truncated concentric zoning pattern (point 8.1 in Fig. 4a), indicative of the metamorphic origin of this and possibly other thin white rims (Hoskin & Black, 2000).

A total of 18 SHRIMP analyses were conducted on 17 different zircons, including one white metamorphic rim and three inherited cores. Fourteen analyses for magmatic zircons showing oscillatory zoning cluster on concordia (Fig. 5a); all of these analyses define a well-constrained mean $^{206}Pb/^{238}U$ age of 446 ± 7 Ma (mean square of weighted deviates (MSWD) = 1.0) that is considered the best estimate for the timing of crystallization of the corresponding intrusion. Three inherited cores (points 3.1, 5.1 and 13.1) plot on or very near concordia and yield Proterozoic ages ranging from 1017 to 1030 Ma. The single rim analysis (point 8.1) gave a $^{206}Pb/^{238}U$ age of 212 ± 12 Ma and may reflect new zircon growth during a later tectonothermal event. It is noteworthy that the analysis of the rim suffers from poor precision because of its extremely high common Pb content ($f_{206} = 12$) and low U (36 ppm) and Th (0.003 ppm) contents (online Appendix Table A1), although it plots on concordia.

4.b. Sample BY005-1: Maofengshan granitic biotite gneiss

Sample BY005-1 was taken from the northern part of the Maofengshan Park area of Guangzhou (23°18′23″N/113°27′23″E) (Fig. 2). This gneiss is composed of approximately 45 % plagioclase ($An_{35–40}$), 32 % quartz, 5 % K-feldspar, 13 % biotite and 5 % sericite, showing an alternation of coarse- and fine-grained mineral bands (Fig. 3b). Biotite is mostly subhedral and fine-grained and sometimes variably chloritized. It makes up weakly orientated flakes, associated with fine-grained feldspar and quartz and defining the main foliation of the rock. Such a microtexture presumably reflects syntectonic recrystallization

https://doi.org/10.1017/S0016756809990811 Published online by Cambridge University Press

under the condition of anistropic stress (Kornprobst, 2002).

This sample contains predominantly elongate zircon grains with length to width ratios between 2:1 and 4:1 (Fig. 4b); approximately 2 % have ratios of 3:2 or are near equant. The zircons range in size between 100 and 350 μm, and are clear and colourless to slightly brown. The CL images reveal concentrically zoned zircon domains of igneous origin, with or usually without relict cores. Many of these oscillatory zoned crystals have a thin white rim (of possibly metamorphic origin) that is inaccessible to ion microprobe spot analysis due to its small scale.

Seventeen analyses were conducted on 17 separate zircon grains with concentric, oscillatory zoning, which is indicative of magmatic crystallization. The analyses are all concordant and have $^{206}Pb/^{238}U$ ratios that are in good agreement within analytical precision (Fig. 5b); the analyses yield a weighted average age of 453.5 ± 7.8 Ma (MSWD = 1.4). We interpret this as the crystallization age of the granitic protolith at Maofengshan.

4.c. Sample BY022-3: granitic biotite gneiss

Sample BY022-3 was collected from an outcrop exposed between Henghe and Ping'an townships in the northeastern corner of the study area (Fig. 2; 23°19′22″N/114°11′39″E), along the northern side of the road to the village of Xiadong. The sample analysed here consists of approximately 35 % quartz, 36 % plagioclase ($An_{35–40}$), 10 % K-feldspar, 18 % biotite, and 1 % sericite. Foliation is defined by biotite that occurs as isolated equant flakes or as partly interconnected networks of flakes. As an effect of retrograde reactions, feldspar is partly replaced by sericite, and biotite by chlorite.

Zircons in the sample are mainly colourless to light brown, but a small proportion of darker brown grains are also present. The size of the crystals varies from less than 100 μm to nearly 420 μm, with the majority of the crystals less than 350 μm in the longest dimension (Fig. 4c). The zircon population of sample BY022-3 is relatively heterogeneous: euhedral, short-prismatic to elongate crystals with relatively sharp edges are most common, but subhedral or anhedral, short-prismatic to equidimensional grains also occur. The CL images show that the euhedral, short-prismatic to elongated grains usually record concentric zoning indicative of igneous growth, whereas subhedral or anhedral grains may be zircons with (e.g. points 6.1 and 15.1, Fig. 4c) or without (e.g. point 9.1, Fig. 4c) a core–rim relationship. Relict cores are more often present, compared to zircons from samples BY004-1 and BY005-1. Very old components (point 1.1, online Appendix Table A1), despite their rarity, are also discovered as unzoned subround whole grains.

Sixteen analyses were performed on 16 zircon grains and include one detrital grain. The complexity of the zircon population is reflected in the ages obtained (Fig. 5c, d; Table 2). Four concordant or near-concordant core analyses (points 6.1, 7.1, 15.1, 16.1) yield Proterozoic ages of 751 to 1190 Ma. Analysis (1.1) plots well away from the concordia line and records a $^{207}Pb/^{206}Pb$ age of 3027 ± 40 Ma, which is the oldest age reported in this region and can be regarded as its minimum age. Of the other 11 analyses, eight were determined on oscillatory-zoned domains of euhedral crystals. They defined a well-constrained concordant mean $^{206}Pb/^{238}U$ age of 439 ± 9 Ma (MSWD = 1.7) (see inset in Fig. 5d), which is regarded as the best estimate for the timing of crystallization of the granitic protolith. The three remaining analyses were determined on bright overgrowths of unzoned zircons (points 8.1, 9.1 and 11.1) that originated possibly from fluid activity during magma crystallization (?), with concordant ages ranging from 401 to 479 Ma. Although similar in Th/U (0.12–0.68) and age to normal magmatic zircons, the three analyses are excluded from the calculation of the weighted mean due to their uncertain significance.

5. $^{40}Ar–^{39}Ar$ thermochronology

K-bearing mineral concentrates from seven rock samples collected from the study area, which include six biotite fractions and one hornblende separate, were used for $^{40}Ar–^{39}Ar$ dating. Hornblende (BY017-22) was derived from a lens of massive amphibolite, whereas biotite samples were obtained from a variety of rock types, including felsic gneiss, micaschist and leucosome. The general sample locations within the Baiyunshan region are shown in Figure 2. It is of note that among the biotite samples, BY005-1 and BY022-3 were extracted from the same hand-specimen as those for U–Pb analyses, and BY017-19 and BY017-25 came from the same quarry site as the analysed hornblende.

The $^{40}Ar/^{39}Ar$ dating results and full analytical data are listed in Table 2 and Appendix Table A2, respectively. Apparent age spectra and, where appropriate, corresponding isotope correlation diagrams (inverse isochrons) are illustrated in Figures 6 and 7 and Appendix Figure A1. The appendices are available as supplementary material online at http://journals.cambridge.org/geo. In the case of hornblende $^{40}Ar/^{39}Ar$ analysis, the K/Ca plot is also included to assist in the interpretation of the spectra.

The standard criterion for identification of plateaux (that is, undisturbed portions of the $^{40}Ar/^{39}Ar$ spectra) is commonly the existence of at least three contiguous steps with concordant ages which contain a significant proportion (> 50 %) of the ^{39}Ar released (Dalrymple & Lanphere, 1974; Dallmeyer & Lecorche, 1990; Lee *et al.* 1991; McDougall & Harrison, 1999). However, a final criterion for defining a 'true plateau' age is based on concordance of inverse-isochron ages defined by isochronous (that is, low MSWD) data and plateau ages (Dalrymple & Lanphere, 1974). In this study, the isochron ages are preferred over the

https://doi.org/10.1017/S0016756809990811 Published online by Cambridge University Press

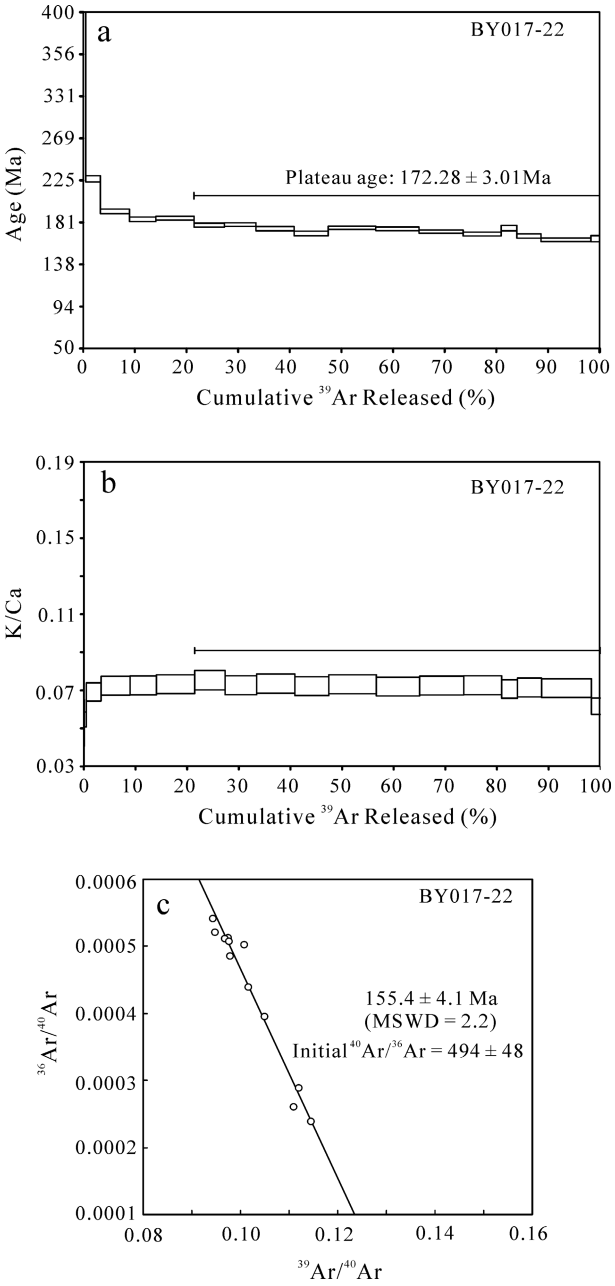

Figure 6. ^{40}Ar–^{39}Ar age spectrum and inverse isochron correlation diagram for hornblende from an amphibolite (BY017-22) collected at Nanxiangshan, showing calculated plateau and isochron ages. Apparent K/Ca spectrum is also presented for this sample. Steps used in the weighted average plateau age are indicated. The steps included in the isochron calculations are the same as those in plateau ages.

plateau ages, since they combine quantitative estimates of analytical precision plus the internal disturbance of the sample and they make no assumption of a present-day ^{40}Ar/^{36}Ar ratio concerning the trapped argon component (e.g. Singer & Pringle, 1996).

5.a. Hornblende

Hornblende from one sample of amphibolite (BY017-22) occurring within the plagioclase–quartz–biotite

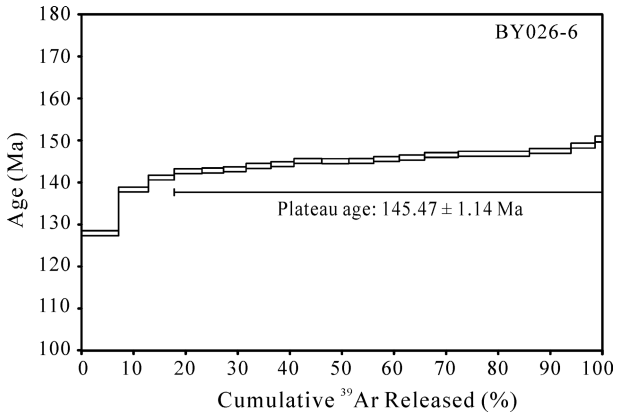

Figure 7. ^{40}Ar–^{39}Ar age spectrum for biotite separated from a mica schist (sample BY026-6) of the Baiyunshan region.

gneiss in the Nanxiangshan Hill displays discordant apparent age spectra (Fig. 6). The low-temperature (or low-laser-power) gas fractions of the spectrum (steps 1–4), comprising < 9.5 % of the ^{39}Ar released, record considerable age variation from *c.* 1903 Ma to < 200 Ma. This situation could occur because of excess ^{40}Ar, phase mixing, and/or ^{39}Ar recoil loss from grain boundaries during irradiation, which produces a high ^{40}Ar/^{39}Ar ratio. In view of the large fluctuation in apparent K/Ca ratios in the low temperature steps (Fig. 6), we conclude that experimental evolution of argon stemmed dominantly from compositionally distinct, relatively Ar-non-retentive phases. Such phases may be represented by (1) very minor, optically undetectable mineralogical contaminants in the hornblende concentrates; (2) petrographically unresolvable exsolution or compositional zonation within constituent hornblende grains (e.g. Siebel, Henjes-Kunst & Rhede, 1998); (3) minor chloritic replacement of hornblende; and/or (4) intracrystalline fluid inclusions (Kelley, 2002; Harrison, Heizler & Lovera, 1993; Harrison *et al.* 1994).

For intermediate- and high-temperature gas fractions that contain 12 of 18 steps and 78.5 % of the ^{39}Ar released, relatively consistent intrasample apparent ^{40}Ar–^{39}Ar ages are obtained, which define a pseudo-plateau date of 172 ± 3 Ma (see below). Because there is little variation in corresponding apparent K/Ca ratios (Fig. 6), the experimental evolution of this part of the extracted gas fractions probably resulted from compositionally uniform sites. These gas fractions generate a ^{36}Ar/^{40}Ar v. ^{39}Ar/^{40}Ar inverse isochron age of 155 ± 4 Ma (MSWD = 2.2) with a poorly constrained initial ^{40}Ar/^{36}Ar ratio of 494 ± 48. The initial ^{40}Ar/^{36}Ar ratio is higher than the present-day atmospheric value (~ 295.5), indicating that small amounts of excess argon were released between steps 7 and 18 and that therefore the apparent ages (calculated assuming ^{40}Ar/^{36}Ar = 295.5) and the resultant plateau age in Figure 6 are not correct. Consequently, only the *c.* 155 Ma isochron age is here considered a geologically significant age. It is interpreted to date the last cooling through temperatures required

https://doi.org/10.1017/S0016756809990811 Published online by Cambridge University Press

for intracrystalline retention of argon in hornblende (~ 500 to 550 °C; e.g. McDougall & Harrison, 1999).

5.b. Biotite

Sample BY005-1 was collected from the Maofengshan orthogneiss. Biotite from this sample gave a 12-step plateau age of 148.76 ± 0.54 Ma (Fig. A1, online Appendix at http://www.cambridge.org/journals/geo). The same temperature steps define an inverse isochron age of 150.3 ± 4.3 Ma (MSWD = 1.7) with an $^{40}Ar/^{36}Ar$ intercept of 255.7 ± 115.8. The ischron age overlaps with the plateau age, taking uncertainties into account, and thus dates the last Ar isotopic closure of the biotite.

Incremental heating of biotite concentrates from three felsic gneisses (BY022-3, BY023-1 and BY017-25) and one leucogranite (BY017-19, locally containing abundant aggregates of biotite) yielded simple apparent age spectra with plateau ages varying between 93.2 ± 0.3 and 97.7 ± 0.4 Ma (Fig. A1, online Appendix). Inverse isochron plots for the biotite analyses result in well-defined ages of 94.0 ± 0.14 Ma ($^{40}Ar/^{36}Ar$ intercept = 282.4 ± 8.3; MSWD = 0.4), 93.6 ± 0.5 Ma ($^{40}Ar/^{36}Ar$ intercept = 281.5 ± 16.6; MSWD = 0.2), 97.5 ± 0.5 Ma ($^{40}Ar/^{36}Ar$ intercept = 304 ± 24; MSWD = 1.5) and 96.3 ± 1.2 Ma ($^{40}Ar/^{36}Ar$ intercept = 257 ± 150; MSWD = 2.7), which are consistent with their respective plateau ages and therefore date the last Ar isotopic closure of the biotite.

Biotite BY026-6 was separated from one mylonitic micaschist from the eastern study area (see Fig. 2 for sample location). A corresponding incremental heating experiment yielded a rising staircase spectrum with no age significance, in which apparent ages increase from 128 to 150 Ma with increasing temperature (Fig. 7; Table A2, online Appendix at http://www.cambridge.org/journals/geo). An insufficient spread in $^{39}Ar/^{40}Ar$ ratios precluded isochron analysis for this sample. Even so, the biotite spectrum is still informative and is in agreement with the diffusional loss of argon (reheating) at ≤ 128 Ma from a biotite that was most likely isotopically reset at ≥ 150 Ma (this time corresponds to a regional tectonothermal event; see Section 6.c). Petrographic observations indicate that the phenocrystic biotite in mylonitic micaschist is strongly deformed and altered to sericite. The deformation and alteration were processes probably responsible for the Ar loss or partial resetting.

6. Discussion

6.a. Intrusion ages of the protoliths of the Baiyunshan gneiss and their implications for the Wuyun Orogeny

U–Pb dating and CL imaging suggest that the zircons in three gneisses from the Baiyunshan Mountains largely formed under magmatic conditions in Late Ordovician to Early Silurian times (*c.* 456–439 Ma, Table 2). This implies a Wuyun igneous origin for the protoliths of most of the felsic gneisses in the region of study. Consequently, the Baiyunshan gneiss cannot represent basement rocks of the Cathaysia Block as previously thought. Our geochronological data contrast with presently widely used geological maps where most of the Baiyunshan gneisses were identified as Sinian or Meso- and Neoproterozoic rocks (Liu & Zhuang, 2003; GBGMR, 1988), but coincides partly with data documented in some earlier literature (Geological Map of Guangzhou, 1968; Geological Map of Heyuan, 1968). On geological maps published in 1968, although the gneiss units (corresponding to BY004-1) are mapped as pre-Devonian metasediments, those (corresponding to BY005-1 and BY022-3) at Maofengshan and some other areas such as Henghe, Ping'an and Boluo are shown as Wuyun intrusions (Fig. 2).

The zircon population in the Maofengshan orthogneiss (BY005-1) constrains the emplacement age of the magmatic protolith to 455.8 ± 6.4 Ma; the granitic orthogneiss thus constitutes the oldest known igneous unit confirmed from Baiyunshan. This emplacement age agrees within error with the age determined for sample BY004-1 of 446 ± 7 Ma; the latter age is also indistinguishable from the zircon formation age (439 ± 9 Ma) for the BY022-3 gneiss from the eastern study area. Therefore, granitic protoliths of the Baiyunshan gneisses can be interpreted to form within a single, continuous, protracted tectonothermal event lasting about 17 Ma. It should be emphasized that the 439 ± 9 Ma age for BY022-3 is slightly younger than that for the foliated Maofengshan granite. Interestingly, BY022-3 is also the sample that contains abundant detrital zircons or inherited cores relative to the other samples. We thus consider it most likely that the 439 ± 9 Ma time corresponds to the waning phase of the Wuyun tectonothermal event.

Our new age constraint for Wuyun magmatism in the Baiyunshan region (the middle segment of the Wuyun Orogen), combined with available geochronological data from southwestern and northeastern sectors of the orogen (Table 1; Fig. 1), indicates that the ages of large amounts of the Wuyun granitoids cluster at *c.* 460–420 Ma in the entire Wuyun Orogen (Table 1; Li *et al.* 1989; Li, 1994; Lou *et al.* 2005; Wang *et al.* 2007*a*; Zhou *et al.* 1994*a*; Peng *et al.* 2006; Li *et al.* 2010; this study). This broad age cluster can be reasonably interpreted to reflect orogen-wide magmatism during this period. Most recent studies have demonstrated that metamorphic overprinting was widespread during the same time interval (Yu *et al.* 2005; Xu *et al.* 2005; Wan *et al.* 2007; Li *et al.* 2010). In addition, it is noted that a transpressive regime initiated its main activity by *c.* 420 Ma in the Wuyi Mountains area (Shu *et al.* 1999) and the Jiangnan belt (see Charvet *et al.* 1996). Therefore, we conclude that the 460–420 Ma magmatism is for the most part syn-orogenic relative to the Wuyun Orogeny.

https://doi.org/10.1017/S0016756809990811 Published online by Cambridge University Press

Syn- to late orogenic magmatic activity in the western segment of the Wuyun Orogen, extending to 402 Ma in the Laojunshan–Song Chay metamorphic dome, appears to terminate later than in its eastern section (Table 1; Li *et al.* 2010). On the orogen scale, however, it is unknown whether Wuyun magmatism was continuous or was composed of discrete magmatic pulses. We want to emphasize that although many ages have been obtained from the Wuyun Orogen, details of the history of magmatic activity are far from being resolved. Further work is needed to refine the timing, duration and migration of magmatic activity of the Wuyun Orogen.

6.b. Sources of Wuyun magmatism

Relict cores in zircon from the Baiyunshan gneiss are abundant and define two clusters of (near-) concordant ages, one with latest Mesoproterozoic ages, including 1030, 1023, 1189 and 1017 Ma, the other with middle Neoproterozoic ages of 762, 751 and 809 Ma. When pooled together, the old age data (excluding 1189 Ma) give a well-constrained weighted $^{206}Pb/^{238}U$ date of 1023 ± 17 Ma (MSWD = 0.21), whereas the younger ones yield a weighted mean age of 772 ± 28 Ma (MSWD = 1.09). Moreover, one of the zircon grains (Table A1, online Appendix at http://www.cambridge.org/journals/geo, analysis 1.1 for BY022-3) yields a discordant SHRIMP analysis, showing that it is a detrital component with minimum age of 3027 Ma. These older zircon components are apparently exotic relative to the Wuyun magmatic stage. They may reflect an anatectic origin of the crustal source rock or country rock assimilation during magma ascent. None the less, the fact that the number of inherited cores is generally large does not support the latter possibility; the amount of assimilation required would demand very high extents of superheating of the magma.

Inherited zircons represent earlier igneous and/or metamorphic phases, the latter of which may be due to reactions (Fraser, Ellis & Eggins, 1997) or recrystallization (Hoskin & Black, 2000). Associated grains dated in this study have variable and high Th/U (0.05–1.34), characteristics that are not typical of zircon grown during prograde metamorphism (online Appendix Table A1; Rubatto, 2002; Hoskin & Schaltegger, 2003). We note that the 1189 Ma to 1017 Ma age range of inherited zircons corresponds to the time of the Sibao Orogeny (*c.* 1.1–0.9 Ga) that formed the South China Block (e.g. Li *et al.* 2002, 2006; Ye *et al.* 2007), and the youngest age cluster at *c.* 772 Ma of inherited zircons is consistent with the period of subsequent intracontinental rifting (830–600 Ma) in the South China Block (e.g. Li *et al.* 1999, 2003; Wang *et al.* 2003*b*; Zhou *et al.* 2007). Thus, despite limited data from the present study, the Baiyunshan orthogneiss can be inferred to have sampled a crustal basement containing significant igneous (or recycled?) components linked to the Rodinia amalgamation and break-up, up to now clearly demonstrated in some other parts of the Wuyi Orogen (e.g. Xu *et al.* 2005; Wan *et al.* 2007). This inference is compatible with the intracontinental nature of the Wuyun Orogeny (e.g. Li *et al.* 2010).

6.c. Late and post-Wuyun tectonothermal history

In the present state of knowledge, it is unclear whether or not the granitic protoliths of the Baiyunshan gneiss underwent a late-Wuyun history of metamorphism and deformation. However, as regional metamorphism and deformation probably continued until *c.* 370 Ma in the Wuyun Orogen (Table 1), we cannot rule out the possibility that solidified Wuyun igneous rocks were syntectonically metamorphosed. By contrast, the Indosinian metamorphic history of the studied felsic gneisses can be constrained by zircon geochronology. Despite the general occurrence of white thin rims that are characteristic of metamorphic zircons (Hoskin & Black, 2000), these could not be analysed in most cases. One exception is in spot 8.1 of sample BY004-1 (Fig. 4a), which gave a $^{206}Pb/^{238}U$ age of 212 ± 12 Ma that may represent the timing of new zircon growth during a later Indosinian tectonothermal event. It therefore remains possible that some of the thinner CL-white rims are also Indosinian in age, as found in (pre-)Wuyun crystalline rocks in the Yunkai Massif and Wuyishan metamorphic belt (Wang *et al.* 2007*a*; Yu *et al.* 2005, 2006; Wan *et al.* 2007). Thus, the present metamorphic age of 212 Ma seems to testify further to a significant influence of the Indosinian tectonothermal event on the continental crust of south China.

Within analytical uncertainty, the biotite $^{40}Ar–^{39}Ar$ age (150 ± 4 Ma, BY005-1) of the Maofengshan pluton overlaps with that of hornblende (155 ± 4 Ma, BY017-22) from an amphibolite lens in Nanxiangshan Hill (Table 2). The $^{40}Ar–^{39}Ar$ age of 155–150 Ma is consistent with the precise zircon U–Pb dates for widely developed early Yanshanian granitic intrusions in Baiyunshan and its neighbouring areas (Figs 1, 2; Liu *et al.* 2005; Li *et al.* 2007; D. S. Yang, unpub. data). Hence, we conclude that the regional magmatic heat in Late Jurassic times caused widespread thermal resetting of the K–Ar isotope system within older high-grade rocks in the Baiyunshan region. This conclusion is also in accord with a 150 Ma apparent age in the last heating step of biotite BY026-6 from mylonitic micaschist that possibly reflects a relict record of a ≥ 150 Ma tectonothermal event, as noted earlier (Fig. 7).

Four younger but similar biotite $^{40}Ar–^{39}Ar$ ages of 94.0 ± 0.14, 93.6 ± 0.5, 97.5 ± 0.5 and 96.3 ± 1.2 Ma have been obtained from gneisses BY022-3, BY023-1 and BY017-25 and leucosome BY017-19 (the latter two samples were from the same quarry site at Nangxiangshan as the hornblende BY017-22) (Fig. 2; Table 2). Regionally, 90–100 Ma volcanic-intrusive rocks are widespread in southeastern China (e.g. Li, 2000; Zhou & Li, 2000). They have been identified

https://doi.org/10.1017/S0016756809990811 Published online by Cambridge University Press

confidently in western and northern Guangdong (e.g. GBGMR, 1988; Geng *et al.* 2006), but have seldom been investigated in central Guangdong. It remains unclear whether the 90–100 Ma magmatism has significantly affected the Baiyunshan region. Thus, the younger ^{40}Ar–^{39}Ar age group can be attributed to either cooling through the biotite closure temperature of approximately 300 to 350 °C (McDougall & Harrison, 1999) or a second resetting of biotite Ar isotopes at *c.* 94–98 Ma due to contemporaneous magmatic activity. Note that in the latter case, the argon system in hornblende cannot have been reset, given the large age difference between hornblende and biotites from Nangxiangshan.

Our present ^{40}Ar–^{39}Ar data reveal that the orthogneiss unit at Maofengshan had already cooled down to about 300 °C at *c.* 150 Ma, but the other studied metamorphic rocks were still at temperatures above ~300 °C until about 90–100 Ma, or were sufficiently heated to reset Ar–Ar ages in biotites at this time, with subsequent rapid cooling to below ~300 °C. The period from 155 Ma to 90 Ma coincides with Late Jurassic to Tertiary extensional shearing along the Xintang–Luofushan detachment fault system (Fig. 2; Wu, Liu & Liao, 2001), implying extensional exhumation of mid-crustal amphibolite-facies rocks during this period. On the basis of the present age data and previous structural investigation (Wu, Liu & Liao, 2001), we suggest that the Maofengshan orthogneiss was exhumed to 8 to 10 >km crustal levels beneath Baiyunshan at *c.* 150 Ma, whereas the eastward components of the gneissic rock masses might have passed upward through the same crustal depth synchronously or later (by *c.* 94 Ma).

Exhumation of middle crustal-level rocks in Baiyunshan since *c.* 155 Ma is roughly coeval with exhumation of gneissic rocks from elsewhere in the Cathaysia Block. To the southwest, a recent fission track analysis of zircon and apatite from the Yunkai terrane shows that the old crystalline basements have been exhumed largely owing to orogenic uplift since Early Cretaceous (Li *et al.* 2005). Based on the *P–T–t* path of isothermal decompression, exhumation of the granulite-facies metamorphic rocks from the Wuyi Mountains area in the eastern Nanling Ranges is considered to be related to Mesozoic extension (Yu *et al.* 2003). This synchroneity reflects the regional Yanshanian tectonic regime characterized by intracontinental lithospheric extension (Li, 2000; Wang *et al.* 2003*c*).

7. Conclusions

Our SHRIMP zircon U–Pb geochronological data indicate that most of the felsic gneisses from the Baiyunshan region cannot represent basements rocks of the Cathaysia Block as previously thought, because of their Late Ordovician–Early Silurian (454–439 Ma) ages, interpreted as the crystallization age of magmatic zircon. Felsic protoliths of the investigated gneisses may have formed within a single, continuous, protracted tectonothermal event lasting about 17 Ma. An integration of available age data for the Wuyun events reflects the emergence of orogen-wide magmatism that could be syn-orogenic and have occurred mainly between 460 and 420 Ma. Inherited zircon studies reveal that the protolith of the Baiyunshan orthogneiss was derived from a crustal basement containing significant igneous or recycled components linked to the Rodinia amalgamation and break-up. A SHRIMP date of 212 Ma from a metamorphic rim of zircon provides evidence for overprinting of a Indosinian tectonothermal event on the Baiyunshan gneiss.

Incremental heating experiments of biotite (6) and hornblende (1) separates from a variety of metamorphic rocks yielded two distinct ^{40}Ar–^{39}Ar age groups: 150–155 and 94–98 Ma. The older ages most likely reflect Late Jurassic magmatism-induced thermal resetting of the K–Ar system, whereas the young age records cooling through the biotite closure temperature of about 300–350 °C or a second resetting of biotite Ar isotopes at *c.* 94–98 Ma. The Maofengshan orthogneiss was exhumed to 8–10 km crustal levels at *c.* 150 Ma, whereas the eastward components of gneissic rock masses appear to have passed upward through the same crustal depth later (by *c.* 94 Ma). Exhumation of middle crustal-level rocks in Baiyunshan since *c.* 155 Ma was roughly coeval with exhumation of gneissic rocks from elsewhere in the Wuyun Orogen, suggesting a large-scale mechanism for the exhumation pulse in Yanshanian times.

Acknowledgements. We thank He-Ping Zou for assistance in the field and Hua-Ning Qiu, Yu-Ruo Shi, Xuan-Ce Wang and Hui-Qing Huang for analytical support. This study was supported by the Chinese National 973 Program (grant 2007CB411403) and the National Natural Science Foundation of China (grants 40728002 and 40825010). This is contribution No. IS-1131 from GIGCAS.

References

BLACK, L. P., KAMO, S. L., ALLEN, C. M., ALEINIKOFF, J. N., DAVIS, D. W., KORSCH, R. J. & FOUDOULIS, C. 2003. TEMORA 1: a new zircon standard for Phanerozoic U–Pb geochronology. *Chemical Geology* **200**, 155–70.

CHARVET, J., LAPIERRE, H. & YU, Y. 1994. Geodynamic significance of the Mesozoic volcanism of southeastern China. *Journal of Southeast Asian Earth Sciences* **68**, 387–96.

CHARVET, J., SHU, L. S., SHI, Y. S., GUO, L. Z. & FAURE, M. 1996. The building of south China: collision of Yangzi and Cathaysia blocks, problems and tentative answers. *Journal of Southeast Asian Earth Sciences* **13**, 223–35.

CHEN, B. 1992. A study of the Gaozhou-Yunlu metamorphic zones of Yunkai Caledonides. *Journal of Nanjing University* **4**(1), 59–67 (in Chinese with English abstract).

CHEN, J. F., FOLAND, K. A., XING, F. M., XU, X. & ZHOU, T. X. 1991. Magmatism along the southeast margin of the Yangtze and Cathaysia Blocks of China. *Geology* **19**, 815–18.

https://doi.org/10.1017/S0016756809990811 Published online by Cambridge University Press

CHEN, J. F. & JAHN, B. M. 1998. Crustal evolution of Southeastern China: Nd and Sr evidence. *Tectonophysics* **284**, 101–33.

DALLMEYER, R. D. & LECORCHE, J. P. 1990. $^{40}Ar/^{39}Ar$ polyorogenic mineral age record in the northern Mauritanide orogen, West Africa. *Tectonophysics* **177**, 81–107.

DALRYMPLE, G. B. & LANPHERE, M. A. 1974. $^{40}Ar/^{39}Ar$ age spectra of some undisturbed terrestrial samples. *Geochimica et Cosmochimica Acta* **38**, 715–38.

DA SILVA, L. C., HARTMANN, L. A., MCNAUGHTON, N. J. & FLETCHER, I. 2000. Zircon U–Pb SHRIMP dating of a Neoproterozoic overprint in Paleoproterozoic granitic-gneissic terranes, southern Brazil. *American Mineralogist* **85**, 649–67.

DENG, J. R. & ZHANG, Z. P. 1996. Study on the Nappe Structure of Xuefeng Old Land in Caledonian Stage in Hunan Province. *Journal of East China Geological Institute* **19**(3), 201–10 (in Chinese with English abstract).

FRASER, G., ELLIS, D. & EGGINS, S. 1997. Zirconium abundance in granulite-facies minerals, with implications for zircon geochronology in high-grade rocks. *Geology* **25**, 607–10.

GAO, S., LIN, W. L. & QIU, Y. M. 1999. Contrasting geochemical and Sm–Nd isotopic compositions of Archaean metasediments from the Kongling high grade terrain of the Yangtze craton: evidence for cratonic evolution and redistribution of REE during crustal anatexis. *Geochimica et Cosmochimica Acta* **63**, 2071–88.

GENG, H. Y., XU, X. S., O'REILLY, S. Y., ZHAO, M. & SUN, T. 2006. Cretaceous volcanic-intrusive magmatism in western Guangdong and its geological significance. *Science in China (Series D)* **49**, 696–713.

GEOLOGICAL MAP OF GUANGZHOU. 1968. Guangdong, People's Republic of China, 1 sheet, scale 1/200,000.

GEOLOGICAL MAP OF HEYUAN. 1968. Guangdong, People's Republic of China, 1 sheet, scale 1/200,000.

GRADSTEIN, F. M., OGG, J. G., SMITH, A. G., BLEEKER, W. & LOURENS, L. J. 2004. A new geologic time scale, with special reference to Precambrian and Neogene. *Episodes* **27**, 83–100.

GBGMR (GUANGDONG BUREAU OF GEOLOGY AND MINERAL RESOURCES). 1988. *Regional Geology of Guangdong Province*, pp. 607–63. Beijing: Geological Publishing House.

GUO, L. G., LIU, Y. P., LI, C. Y., XU, W. & YE, L. 2009. SHRIMP zircon U–Pb geochronology and lithogeochemistry of Caledonian Granites from the Laojunshan area, southeastern Yunnan province, China: Implications for the collision between the Yangtze and Cathaysia blocks. *Geochemical Journal* **43**, 101–22.

GUO, L. Z., SHI, Y. S., LU, H. F., MA, R. S. & DONG, H. G. 1989. The pre-Devonian tectonic patterns and evolution of south China. *Journal of Southeast Asian Earth Sciences* **3**(1–4), 87–93.

GUO, L. Z., YU, J. H. & SHI, Y. S. 1965. Main features of tectonic development of the Caledonian period folded geosyncline, south China. In *Geotectonic Problems of China*, pp. 165–83. Beijing: Science Press.

HANCHAR, J. M. & MILLER, C. F. 1993. Zircon zonation patterns as revealed by cathodoluminescence and backscattered electron images: implications for interpretation of complex crustal histories. *Chemical Geology* **110**, 1–13.

HARRISON, T. M., HEIZLER, M. T. & LOVERA, O. M. 1993. In vacuo crushing experiments and K-feldspar thermochronology. *Earth and Planetary Science Letters* **117**, 169–80.

HARRISON, T. M., HEIZLER, M. T., LOVERA, O. M., CHEN, W. & GROVE, M. 1994. A chlorine disinfectant for excess argon released from K-feldspar during step heating. *Earth and Planetary Science Letters* **123**, 95–104.

HOSKIN, P. W. O. & BLACK, L. P. 2000. Metamorphic zircon formation by solid-state recrystallization of protolith igneous zircon. *Journal of Metamorphic Geology* **18**, 423–39.

HOSKIN, P. W. O. & SCHALTEGGER, U. 2003. The composition of zircon and igneous and metamorphic petrogenesis. *Reviews in Mineralogy and Geochemistry* **53**, 27–62.

HSÜ, K. J. 1994. Tectonic facies in an archipelago model of intra-plate orogenesis. *Geological Society of America Today* **4**, 289–93.

HUANG, T. K. 1960. The main characteristics of the geologic structures of China: preliminary conclusions. *Acta Geologica Sinica* **40**(1), 1–37.

JAHN, B. M., ZHOU, X. H. & LI, J. L. 1990. Formation and tectonic evolution of southeastern China and Taiwan: Isotopic and geochemical constraints. *Tectonophysics* **183**, 145–60.

KELLEY, S. 2002. Excess argon in K–Ar and Ar–Ar geochronology. *Chemical Geology* **188**, 1–22.

KOPPERS, A. A. P. 2002. ArArCALC-software for $^{40}Ar/^{39}Ar$ age calculations. *Computers & Geosciences* **28**, 605–19.

KORNPROBST, J. 2002. *Metamorphic Rocks and Their Geodynamic Significance – A Petrological Handbook*. Dordrecht: Kluwer Academic Publishers.

LAPIERRE, H., JAHN, B. M., CHARVET, J. & YU, Y. W. 1997. Mesozoic magmatism in Zhejiang Province and its relation with the tectonic activities in SE China. *Tectonophysics* **274**, 321–38.

LEE, J. K. W., ONSTOTT, T. C., CASHMAN, K. V., CUMBEST, R. J. & JOHNSON, D. 1991. Incremental heating of hornblende in vacuo: Implications for $^{40}Ar/^{39}Ar$ geochronology and the interpretation of thermal histories. *Geology* **19**, 872–6.

LI, X. H. 1994. A comprehensive U–Pb, Sm–Nd, Rb–Sr and ^{40}Ar–^{39}Ar geochronological study on Guidong Granodiorite, southeast China: Records of multiple tectonothermal events in a single pluton. *Chemical Geology* **115**, 283–95.

LI, X. H. 1997. Timing of the Cathaysia Block formation: Constraints from SHRIMP U–Pb zircon geochronology. *Episodes* **20**, 188–92.

LI, X. H. 2000. Cretaceous magmatism and lithospheric extension in southeast China. *Journal of Asian Earth Sciences* **18**, 293–305.

LI, X. H., LI, Z. X., WINGATE, M. T. D., CHUNG, S. L., LIU, Y., LIN, G. C. & LI, W. X. 2006. Geochemistry of the 755 Ma Mundine Well dyke swarm, northwestern Australia: part of a Neoproterozoic mantle superplume beneath Rodinia? *Precambrian Research* **146**, 1–15.

LI, X. H.., LI, Z. X., LI, W. X., LIU, Y., YUAN, C., WEI, G. J. & QI, C. S. 2007. U–Pb zircon, geochemical and Sr–Nd–Hf isotopic constraints on age and origin of Jurassic I- and A-type granites from central Guangdong, SE China: A major igneous event in response to foundering of a subducted flat-slab? *Lithos* **96**, 186–204.

LI, X. H. & MCCULLOCH, M. T. 1996. Secular variations in the Nd isotopic composition of the Neoproterozoic sediments from the southern margin of the Yangtze Block: evidence for a Proterozoic continental collision in southeastern China. *Precambrian Research* **76**, 67–76.

LI, X. H., TATSUMOTO, M., PREMO, W. R. & GUI, X. T. 1989. Age and origin of the Tanghu granite, southeast China: results from U–Pb single zircon and Nd isotopes. *Geology* **17**, 395–9.

LI, X. M., WANG, Y. J., TAN, K. X. & PENG, T. P. 2005. Meso-Cenozoic uplifting and exhumation on Yunkaidashan: Evidence from fission track thermochronology. *Chinese Science Bulletin* **50**(9), 903–9.

LI, Z. X. 1998. Tectonic history of the major east Asian lithospheric blocks since the mid-Proterozoic: a synthesis. In *Mantle Dynamics and Plate Interactions in East Asia, Geodynamics Series 27* (eds F. J. Martin, S. L. Chung, C. H. Lo & T. Y. Lee), pp. 221–43. American Geophysical Union.

LI, Z. X. & LI, X. H. 2007. Formation of the 1300 km-wide intra-continental orogen and post-orogenic magmatic province in Mesozoic South China: A flat-slab subduction model. *Geology* **35**, 179–82.

LI, Z. X., LI, X. H., KINNY, P. D. & WANG, J. 1999. The Breakup of Rodinia: Did it start with a mantle plume beneath south China? *Earth and Planetary Science Letters* **173**, 171–81.

LI, Z. X., LI, X. H., KINNY, P. D., WANG, J., ZHANG, S. & ZHOU, H. 2003. Geochronology of Neoproterozoic syn-rift magmatism in the Yangtze Craton, South China and correlations with other continents: evidence for a mantle superplume that broke up Rodinia. *Precambrian Research* **122**, 85–109.

LI, Z. X., LI, X. H., WARTHO, J. A., CLARK, C., LI, W. X., ZHANG, C. L. & BAO, C. M. 2010. Magmatic and metamorphic events during the Early Paleozoic Wuyi-Yunkai Orogeny, southeastern South China: New age constraints and P–T conditions. *Geological Society of America Bulletin*, DOI 10.1130/B30021.1, in press.

LI, Z. X., LI, X. H., ZHOU, H. & KINNY, P. D. 2002. Grenvillian continental collision in south China: new SHRIMP U–Pb zircon results and implications for the configuration of Rodinia. *Geology* **30**, 163–6.

LI, Z. X. & POWELL, C. M. 2001. An outline of the Paleogeographic evolution of the Australasian region since the beginning of the Neoproterozoic. *Earth-Science Reviews* **53**, 237–77.

LIU, B. & XU, X. (eds) 1994. *Atlas of Lithofacies and Paleogeography of South China*. Beijing: Science Press, 188 pp.

LIU, C. S., CHEN, X. M., WANG, R. C., ZHANG, A. C. & HU, H. 2005. The products of partial melting of the lower crust: origin of early Yanshanian Lapu monzogranite, Guangdong province. *Geological Journal of China Universities* **11**, 343–57.

LIU, J. X. & ZHUANG, W. M. 2003. Zircon Pb–Pb ages of Pre-Sinian basement in central Guangdong Province and their geological significance. *Geology and Mineral Resources of South China* **2**, 52–7 (in Chinese with English abstract).

LIU, R., ZHANG, L., ZHOU, H. W., ZHONG, Z. Q., ZENG, W., XIANG, H., JIN, S., LU, X. Q. & LI, C. Z. 2008. Petrogenesis of the Caledonian migmatites and related granites in northwestern Fujian province, south China: syn-deformational crustal anatexis. *Acta Petrologica Sinica* **24**(6), 1205–22 (in Chinese with English abstract).

LOU, F. S., SHEN, W. Z., WANG, D. Z., SHU, L. S., WU, F. J., ZHANG, F. R. & YU, J. H. 2005. Zircon U–Pb chronology of the Wugongshan dome compound granite in Jiangxi province. *Acta Geologica Sinica* **79**, 636–44 (in Chinese with English abstract).

MCDOUGALL, I. & HARRISON, M. T. 1999. *Geochronology and thermochronology by the $^{40}Ar/^{39}Ar$ method. Second edition.* New York: Oxford University Press, 269 pp.

MCKERROW, W. S., NIOCAILL, C. M. & DEWEY, J. F. 2000, The Caledonian Orogeny redefined. *Journal of the Geological Society, London* **157**, 1149–54.

PENG, S. B., JIN, Z. M., LIU, Y. H., FU, J. M., HE, L. Q., CAI, M. H. & WANG, Y. B. 2006. Petrochemistry, chronology and tectonic setting of strong peraluminous anatectic granitoids in Yunkai Orogenic Belt, western Guangdong Province, China. *Earth Science – Journal of China University of Geosciences* **17**(1), 1–12.

QIU, H. N. & WIJBRANS, J. R. 2006. Paleozoic ages and excess ^{40}Ar in garnets from the Bixiling eclogite in Dabieshan, China: New insights from $^{40}Ar/^{39}Ar$ dating by stepwise crushing. *Geochimica et Cosmochimica Acta* **70**, 2354–70.

QIU, H. N. 2006. Construction and development of new Ar–Ar laboratories in China: Insight from GV-5400 Ar–Ar laboratory in Guangzhou Institute of Geochemistry, Chinese Academy of Sciences. *Geochimica* **35**, 133–40 (in Chinese with English abstract).

REN, J. S. 1964. A preliminary study on pre-Devonian geotectonic problems of southeastern China. *Acta Geologica Sinica* **44**(4), 418–31.

ROGER, F., LELOUP, P. H., JOLIVET, M., LACASSIN, R., TRINH, P. T., BRUNEL, M. & SEWARD, D. 2000. Long and complex thermal history of the Song Chay metamorphic dome (Northern Vietnam) by multi-system geochronology. *Tectonophysics* **321**, 449–66.

RUBATTO, D. 2002. Zircon trace element geochemuistry: Partitioning with garnet and the link between U–Pb ages and metamorphism. *Chemical Geology* **184**, 123–38.

SANG, H. Q., WANG, F, HE, H. Y., WANG, Y. L., YANG, L. K. & ZHU, R. X. 2006. Intercalibration of ZBH-25 biotite reference material utilized for K–Ar and ^{40}Ar–^{39}Ar age determination. *Acta Petrologica Sinica* **22**(12), 3059–78.

SHEN, W. Z., LING, H. F., LI, W. X. & WANG, D. Z. 2000. Crust evolution in southeast China: evidence from Nd model ages of granitoids. *Science in China* **43**, 36–49.

SHUI, T., XU, B. T., LIANG, R. H. & QIU, Y. S. 1986. Shaoxing–Jiangshan deep-seated fault zone, Zhejiang province. *Chinese Science Bulletin* **81**(18), 1250–5.

SIEBEL, W., HENJES-KUNST, F. & RHEDE, D. 1998. High-temperature memory in calcic amphiboles and constraints on compositional control of their $^{40}Ar/^{39}Ar$ ages. *Geology* **26**, 31–4.

SHU, L. S. 2006. Predevonian tectonic evolution of south China: from Cathaysian Block to Caledonian period folded orogenic belt. *Geological Journal of China Universities* **12**, 418–31.

SHU, L. S., LU, H. F., JIA, D., CHARVET, J. & FAURE, M. 1999. Study of the $^{40}Ar/^{39}Ar$ isotopic age for the early Paleozoic tectonothermal event in the Wuyishan region, south China. *Journal of Nanjing University (Natural Sciences)* **35**, 668–74 (in Chinese with English abstract).

SINGER, B. S. & PRINGLE, M. S. 1996. Age and duration of the Matuyama-Brunhes geomagnetic polarity reversal from $^{40}Ar/^{39}Ar$ incremental heating analyses of lavas. *Earth and Planetary Science Letters* **139**, 47–61.

STEIGER, R. H. & JÄGER, E. 1977. Subcommission on geochronology: convention on the use of decay constants in geo- and cosmochronology. *Earth and Planetary Science Letters* **36**, 359–62.

SUN, T. 2006. A new map showing the distribution of granites in South China and its explanatory notes. *Geological Bulletin of China* **25**, 332–5.

WAN, Y. S., LIU, D. Y., XU, M. H., ZHUANG, J. M., SONG, B., SHI, Y. R. & DU, L. L. 2007. SHRIMP U–Pb zircon geochronology and geochemistry of metavolcanic and metasedimentary rocks in northwestern Fujian, Cathaysia block, China: Tectonic implications and the need to redefine lithostratigraphic units. *Gondwana Research* **12**(1–2), 166–83.

WANG, H. N., LING, H. F., ZHOU, L. Y., YANG, F. G. & WANG, Y. X. 2003*a*. Sm–Nd isotope dating and geological implications for the Mesoproterozoic Manmianshan Group in Fujian province. *Geological Journal of China Universities* **9**(4), 566–72.

WANG, J., LI, X. H., DUAN, T. Z., LIU, D. Y., SONG, B., LI, Z. X. & GAO, Y. H. 2003*b*. Zircon SHRIMP U–Pb dating for the Cangshuipu volcanic rocks and its implications for the lower boundary age of the Nanhua strata in South China. *Chinese Science Bulletin* **48**, 1663–9.

WANG, Y. J., FAN, W. M., GUO, F., PENG, T. P. & LI, C. W. 2003*c*. Geochemistry of Mesozoic mafic rocks around the Chenzhou–Linwu fault in south China: implication for the lithospheric boundary between the Yangtze and the Cathaysia Blocks. *International Geology Review* **45**, 263–86.

WANG, J. & LI, Z. X. 2003. History of Neoproterozoic rift basins in South China: implications for Rodinia break-up. *Precambrian Research* **122**, 141–58.

WANG, J. H., TU, X. L. & SUN, D. Z. 1999. U–Pb dating of anatectic migmatites at Gaozhou in the Yunkai block, western Guangdong, China. *Geochimica* **28**(3), 231–8 (in Chinese with English abstract).

WANG, Y. J., FAN, W. M., ZHAO, G. C., JI, S. C. & PENG, T. P. 2007*a*. Zircon U–Pb geochronology of gneissic rocks in the Yunkai massif and its implications on the Caledonian event in the South China Block. *Gondwana Research* **12**, 404–16.

WANG, Y. J., FAN, W. M., SUN, M., LIANG, X. Q., ZHANG, Y. H. & PENG, T. P. 2007*b*. Geochronological, geochemical and geothermal constraints on petrogenesis of the Indosinian peraluminous granites in the South China Block: A case study in the Hunan Province. *Lithos* **96**, 475–502.

WIJBRANS, J. R., PRINGLE, M. S., KOPPERS, A. A. P. & SCHEVEERS, R. 1995. Argon geochronology of small samples using the Vulkaan Argon laser-probe. *Proceedings of the Koninklijke Nederlandse Akademie Van Wetenschappen–Biological Chemical Geological Physical and Medical Sciences* **98**(2), 185–218.

WILLIAMS, I. S. 1998. U–Th–Pb geochronology by ion microprobe. In *Applications of microanalytical techniques to understanding mineralizing processes* (eds M. A. McKibben, W. C. Shanks III & W. I. Ridley), pp. 1–35. *Reviews of Economic Geology* **7**.

WU, J. T., LIU, J. X. & LIAO, S. T. 2001. Basic features of detachment fault in southwest section of the Heyuan fault zone. *Guangdong Geology* **16**(4), 40–7 (in Chinese with English abstract).

WU, Q. Z. 1991. New materials and viewpoint on the strata in Guangzhou district. *Guangdong Geology* **6**(1), 43–52 (in Chinese with English abstract).

XU, B., GUO, L. Z. & SHI, Y. S. 1992. *The Proterozoic terranes and mutiphase collision-orogens in Anhui–Zhejiang–Jiangxi area*. Beijing: Geological Publishing House (in Chinese with English abstract).

XU, X. S., O'REILLY, S. Y., GRIFFIN, W. L., DENG, P. & PEARSON, N. J. 2005. Relict Proterozoic basement in the Nanling Mountains (SE China) and its tectonothermal overprinting. *Tectonics* **24**, TC2003.

YAN, D. P., ZHOU, M. F. & WANG, Y. C. 2006. Structural and geochronological constraints on the Dulong–Song Chay tectonic dome in SE Yunnan (SW China) and northern Vietnam. *Journal of Asian Earth Sciences* **28**, 332–53.

YE, M. F., LI, X. H., LI, W. X., LIU, Y. & LI, Z. X. 2007. SHRIMP zircon U–Pb geochronological and whole-rock geochemical evidence for an early Neoproterozoic Sibaoan magmatic arc along the southeastern margin of the Yangtze Block. *Gondwana Research* **12**, 144–56.

YE, Y., LAN, Y. Q., CHEN, Y. S. & EDWARD, F. 1994. ^{40}Ar–^{39}Ar chronology and metamorphic age of Chencai Group, Zhejiang province, China. *Acta Petrologica Sinica* **10**(2), 193–201.

YU, J. H., WANG, L. J., ZHOU, X. M., JIANG, S. Y., WANG, R. C., XU, X. S. & QIU, J. S. 2006. Compositions and formation history of the basement metamorphic rocks in northeastern Guangdong province. *Earth Science – Journal of China University of Geosciences* **31**, 38–48 (in Chinese with English abstract).

YU, J. H., ZHOU, X. M., O'REILLY, Y. S., ZHAO, L., GRIFFIN, W. L., WANG, R. C., WANG, L. J. & CHEN, X. M. 2005. Formation history and protolith characteristics of granulite facies metamorphic rock in Central Cathaysia deduced from U–Pb and Lu–Hf isotopic studies of single zircon grains. *Chinese Science Bulletin* **50**(18), 2080–9.

YU, J. H., ZHOU, X. M., ZHAO, L. & CHEN, X. M. 2003. Discovery and implications of granulite facies metamorphic rocks in the eastern Nanling, China. *Acta Petrologica Sinica* **19**(3), 461–7.

ZENG, W., ZHANG, L., ZHOU, H. W., ZHONG, Z. Q., XIANG, H., LIU, R., JIN, S., LU, X. Q. & LI, C. Z. 2008. Caledonian reworking of Paleoproterozoic basement in the Cathaysia Block: Constraints from zircon U–Pb dating, Hf isotopes and trace elements. *Chinese Science Bulletin* **53**(6), 895–904.

ZHANG, S. G. & WU, J. S. 2002. The metamorphic Geology of China. In *Geological Atlas of China* (ed. L. F. Ma), pp. 28–31. Beijing: Geological Publishing House.

ZHOU, H. W., YOU, Z. D., ZHONG, Z. Q. & HAN, Y. J. 1994*a*. Characteristics of zircons in orbicular gneissic biotite-granite from Yunkai uplifted area. *Earth Science – Journal of China University of Geosciences* **19**(4), 427–32 (in Chinese with English abstract).

ZHOU, H. W., YOU, Z. D., ZHONG, Z. Q. & HAN, Y. J. 1994*b*. New findings of low pressure granulite facies metamorphic age in the Yunkai uplift. *Geological Science and Technology Information* **13**(3), 23–6 (in Chinese with English abstract).

ZHOU, J. B., LI, X. H., GE, W. C. & LI, Z. X. 2007. Age and origin of middle Neoproterozoic mafic magmatism in southern Yangtze Block and relevance to the break-up of Rodinia. *Gondwana Research* **12**, 184–97.

ZHOU, X. M. & LI, W. X. 2000. Origin of Late Mesozoic igneous rocks in Southeastern China: implications for lithosphere subduction and underplating of mafic magmas. *Tectonophysics* **326**, 269–87.

ZHOU, X. M. & ZHU, Y. H. 1992. Magma mixing within the Jiangshan–Shaoxing fault zone and Precambrian geology on both its sides. *Science in China (Series B)* **3**, 296–303 (in Chinese).

ZHOU, X. M., SUN, T., SHEN, W. Z., SHU, L. S. & NIU, Y. L. 2006. Petrogenesis of Mesozoic granitoids and volcanic rocks in South China: A response to tectonic evolution. *Episodes* **29**, 26–33.

ZOU, H. P., QIU, Y. X., ZHUANG, W. M. & SHAO, R. S. 2001. Determination of deformation stages of the Shougouling fault zone in the Guangzhou area. *Regional Geology of China*, **20**(1), 67–72, 81.